Journal Pre-proof

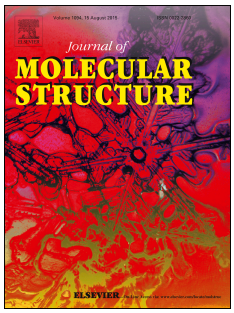

Two new benzamides: Synthesis, spectroscopic characterization, X-ray diffraction, and electronic structure analyses

Başak Koşar Kırca, Şükriye Çakmak, Hasan Yakan, Mustafa Odabaşoğlu, Orhan Büyükgüngör, Halil Kütük

PII: S0022-2860(19)31423-1

DOI: https://doi.org/10.1016/j.molstruc.2019.127314

Reference: MOLSTR 127314

To appear in: *Journal of Molecular Structure*

Received Date: 25 July 2019

Revised Date: 16 October 2019

Accepted Date: 28 October 2019

Please cite this article as: Baş.Koş. Kırca, Şü. Çakmak, H. Yakan, M. Odabaşoğlu, O. Büyükgüngör, H. Kütük, Two new benzamides: Synthesis, spectroscopic characterization, X-ray diffraction, and electronic structure analyses, *Journal of Molecular Structure* (2019), doi: https://doi.org/10.1016/j.molstruc.2019.127314.

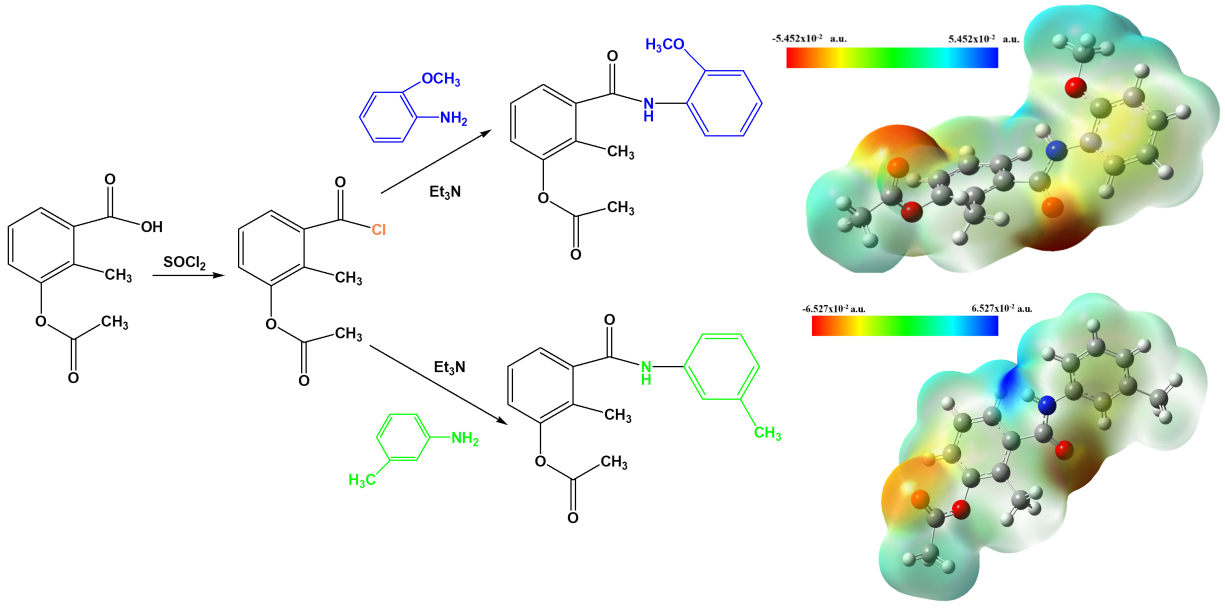
SOCl2
Et3N
Et3N
-5.452x10-2 a.u.
5.452x10-2 a.u.
-6.527x10-2 a.u.
6.527x10-2 a.u.

Two New Benzamides: Synthesis, Spectroscopic Characterization, X-ray Diffraction, and Electronic Structure Analyses

Başak Koşar Kırca[a,*], Şükriye Çakmak[b,*], Hasan Yakan[c], Mustafa Odabaşoğlu[d], Orhan Büyükgüngör[e], Halil Kütük[f]

[a]*Department of Mathematics and Science Education, Sinop University, Sinop, Turkey*

[b]*Environmental Health Programme, Sinop University, Sinop, Turkey*

[c]*Department of Chemistry Education, Ondokuz Mayis University, Samsun, Turkey*

[d]*Chemical Technology Program, Pamukkale University, Denizli, Turkey*

[e]*Department of Physics, Ondokuz Mayis University, Samsun, Turkey*

[f]*Department of Chemistry, Ondokuz Mayis University, Samsun, Turkey*

***Corresponding Author**

Şükriye Çakmak, PhD

Fax : +90 368 287 62 69

Phone: +90 368 287 62 55

E-mail: scakmak@sinop.edu.tr

Address: Environmental Health Programme

Sinop University, Sinop, 57000, Turkey.

Two New Benzamides: Synthesis, Spectroscopic Characterization, X-ray Diffraction, and Electronic Structure Analyses

Başak Koşar Kırca[a,*], Şükriye Çakmak[b,*], Hasan Yakan[c], Mustafa Odabaşoğlu[d], Orhan Büyükgüngör[e], Halil Kütük[f]

[a]*Department of Mathematics and Science Education, Sinop University, Sinop, Turkey*

[b]*Environmental Health Programme, Sinop University, Sinop, Turkey*

[c]*Department of Chemistry Education, Ondokuz Mayis University, Samsun, Turkey*

[d]*Chemical Technology Program, Pamukkale University, Denizli, Turkey*

[e]*Department of Physics, Ondokuz Mayis University, Samsun, Turkey*

[f]*Department of Chemistry, Ondokuz Mayis University, Samsun, Turkey*

Abstract

This work includes the syntheses, molecular and electronic structure analyses of two novel secondary amide compounds 3-acetoxy-2-methyl-*N*-(2-methoxyphenyl)benzamide, **1** and 3-acetoxy-2-methyl-*N*-(3-methylphenyl)benzamide, **2**. The title compounds were characterized by X-ray single crystal diffraction, FT-IR, ^{1}H NMR and ^{13}C NMR techniques and quantum chemical calculations were used for the investigations on electronic structure. X-ray diffraction analyses show that both compounds **1** and **2** crystallized in the triclinic system with space group P-1. While the characteristic amide bands were observed in IR and NMR spectra, crystallographic studies indicate that the supramolecular structures were stabilized by intramolecular and intermolecular hydrogen bonds and C-H…π interactions for both compounds. Beside the experimental studies, natural bond orbital and molecular electrostatic potential analyses were carried out to understand the intramolecular charge transfers and hydrogen bonding behaviors of compounds.

Keywords: Secondary amides, non-covalent interactions, spectroscopic techniques, X-ray diffraction, electronic structure.

1. Introduction

The amide functional group can be found extensively in nature and its great significance is well known. The common features of all the most important biological molecules such as peptides and proteins are that they contain amide functional groups [1-8].

Literature review shows that the amide linkage containing compounds like benzamide derivatives deserve special consideration as they have biological and pharmacological activities such as antibacterials [9, 10], antimicrobial [11], antifungal [12], andanticonvulsant [13] antiinflamatory [14], anti-HSV [15], analgesic [16], antitumor [17], and anticancer [18] among other applications.

Medical and industrial fields make broad use compounds contain the amide functionality [19]. Amides are also widespread in coordination chemistry because of their coordinating ability [20]. Many complexes have been studied with amide group ligands which display various coordinating behavior with diverse metal ions [21].

An increase has recently been seen in quantum chemical computational studies on electronic structure of compounds. Density Functional Theory (DFT) calculations based upon computational quantum chemistry has been shown as favorite among several computational chemistry methods because of its great accuracy in reproducing the experimental values and advantages in designing/characterizing new molecules [22, 23].

Based on this information, we have synthesized some new benzamides which have been described below and investigated with experimental and theoretical methods to elucidate their structures. Cakmak et al. [24] prepared many substituted secondary amide compounds such as 2,3-dimethoxybenzoic acid and aniline derivatives. These new compounds, which include 3-acetoxy-2-methyl-*N*-(4-methoxyphenyl) benzamide, are shown to have great antioxidant properties [25]. The ultimate goal of this article is to outline the synthesis and elucidation of new secondary compounds within the line of our ongoing projects.

2. Experimental procedures

*2.1. Synthesis of 3-acetoxy-2-methyl-N-(2-methoxyphenyl)benzamide (**1**)*

2-methoxyaniline (10 mmol) was dissolved in THF (5 mL), and trimethylamine (1.4 mL, 10 mmol) was added dropwise. Into this reaction, a mixture was slowly added 3-acetoxy-2-methylbenzoyl chloride (2.34 g, 11 mmol) in THF (5 mL) at room temperature. After the reaction mixture was stirred at room temperature for 15 hours, the resulting white salt precipitate was filtered off and then 150 mL water was added dropwise to the filtrate. The precipitate was filtered off and washed several times with water to remove excessive aniline and triethylamine hydrochloride salt. The crude product was crystallized from acetonitrile: methanol (2:1) (2.30 g, 70%; m.p. 128-130℃). The synthesis reaction is given in Scheme 1.

*2.2. Synthesis of 3-acetoxy-2-methyl-N-(3-methylphenyl) benzamide (**2**)*

3-methylaniline (10 mmol) and triethylamine (10 mmol) in THF (10 mL) was added to dropwise solution of 3-acetoxy-2-methylbenzoyl chloride (11 mmol) in THF (10 mL) at room temperature. The reaction mixture was stirred at room temperature for 15 h; next, the resulting white salt precipitate was filtered off, and then 100 mL water was added dropwise to the filtrate. The precipitate was filtered off and washed several times with water to remove excess aniline derivative and trimethylamine hydrochloride salt. The crude product was crystallized from acetonitrile (1.87 g, 60%; m.p. 142-145℃). The synthesis reaction is given in Scheme 1.

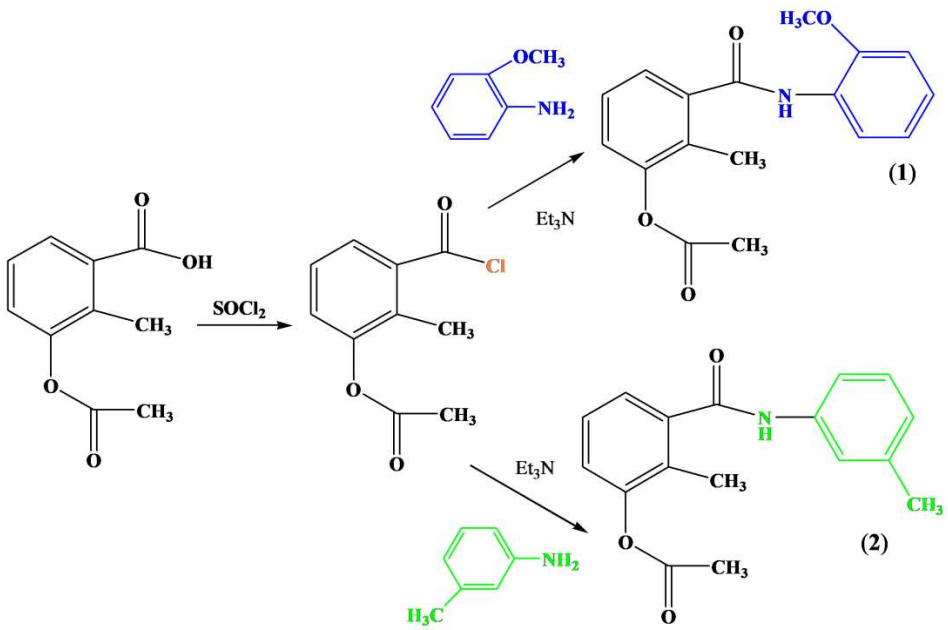

Scheme 1. Synthesis of compunds **1** and **2**.

2.3. Instrumentation

All reagents were purchased from commercial sources (Merck, ABCR, or Sigma-Aldrich) and used without further purification except commercial thionyl chloride. It was fractionally distilled twice to give a colourless product of high purity, b.p. 77 °C/760 mmHg. The solvents were of analytical grade. ^{1}H and ^{13}C NMR spectra were taken at room temperature on a Bruker/Ultraschilt operating at 300 MHz for ^{1}H, and 75 MHz for ^{13}C NMR. IR spectra were recorded with a Bruker Vertex 80V. All melting points were measured with a Stuart SMP 30. X-Ray diffraction data were collected with a STOE IPDS II diffractometer.

2.4. Crystal structure determination

A suitable sample of size 0.66 × 0.38 × 0.07 mm^3 for **1** and 0.80 × 0.29 × 0.03 mm^3 for **2** were chosen for the single crystal X-ray study. Reflections were collected in the rotation mode (ω scanning mode) and cell parameters were determined by using X-AREA software [24]. Absorption corrections (μ_1 = 0.094 mm^{-1} and μ_2 = 0.083 mm^{-1}) were achieved by the integration method via X-RED32 software [26]. The structures were solved by direct methods

using SHELXT-2014/4 [27]. The refinements were carried out by full-matrix least-squares method using SHELXL 2016 on the positional and anisotropic temperature parameters of the non-hydrogen atoms, or equivalently corresponding to 201 crystallographic parameters for **1** and 383 for **2** [28]. All non-hydrogen atom parameters were refined anisotropically and after checking the electron map, H atoms were positioned geometrically and refined using a riding model. The C-H bond distances were fixed to 0.93 Å for CH and 0.96 Å for CH_3 groups. The U_{iso} values of H atoms were also fixed to 1.2 times U_{eq} value of parent atoms for CH and 1.5 times U_{eq} value of parent atoms for CH_3 groups. Under the condition of $I > 2\sigma(I)$ threshold, the structures were refined to R = 0.0415, wR2 = 0.1023, S = 1.042 with 3114 observed reflections for **1** and R = 0.0840, wR2 = 0.1959, S = 0.914 with 6623 observed reflections for **2**. The other data collection conditions and parameters of refinement process are listed in Table 1.

Table 1. Unit cell information, reflection data and refinement details for **1** and**2**.

	1	**2**
Formula	$C_{17}H_{17}NO_4$	$C_{17}H_{17}NO_3$
Formula weight	299.31	283.31
Crystal system	Triclinic	Triclinic
Space group	P-1	P-1
Z	2	2
a (Å)	5.0970(14)	7.6769 (7)
b(Å)	10.907 (2)	8.8152 (8)
c (Å)	13.974 (3)	23.386 (2)
α (°)	77.117 (16)	82.708 (8)
β (°)	85.600 (2)	82.947 (7)
γ (°)	87.360 (2)	89.993 (7)
V ($Å^3$)	754.7 (3)	1557.7 (3)
Radiation type	MoK_α	MoK_α
μ (mm^{-1})	0.094	0.083
T_{max}, T_{min}	0.9873, 0.9912	0.9764, 0.9956
Reflections read	11543	26056
Unique reflections	2402	2101
Refl. with I>2σ(I)	3114	6623

Refined parameters	201	383
θ_{max}, θ_{min}	26.497, 2.680	26.752, 1.769
h, k, l	-6<h<6, -13<k<13, -17<l<17	-9<h<9, -11<k<10, -29<l<29
$R[F_2>2\sigma(F_2)]$	0.0415	0.0840
$wR(F_2)$	0.1023	0.1959
S	1.0420	0.9140

2.5. Supplementary data

CCDC 1472110 for **1** and CCDC 1472112 for **2** contain the supplementary crystallographic data for this paper. These data can be obtained free of charge via www.ccdc.cam.ac.uk/structures, by emailing data_request@ccdc.cam.ac.uk, or by contacting The Cambridge Crystallographic Data Centre, 12, Union Road, Cambridge CB2 1EZ, UK; fax: +44 1223 336033.

3. Results and discussion

3.1. Crystal structures

Fig. 1 and Fig. 2 show the ORTEP-3 [29] plots and atom numbering schemes for the title compounds **1** and **2**. Hydrogens are drawn as small spheres of arbitrary radii and the other atoms are seen as displacement ellipsoids at 30% probability level.

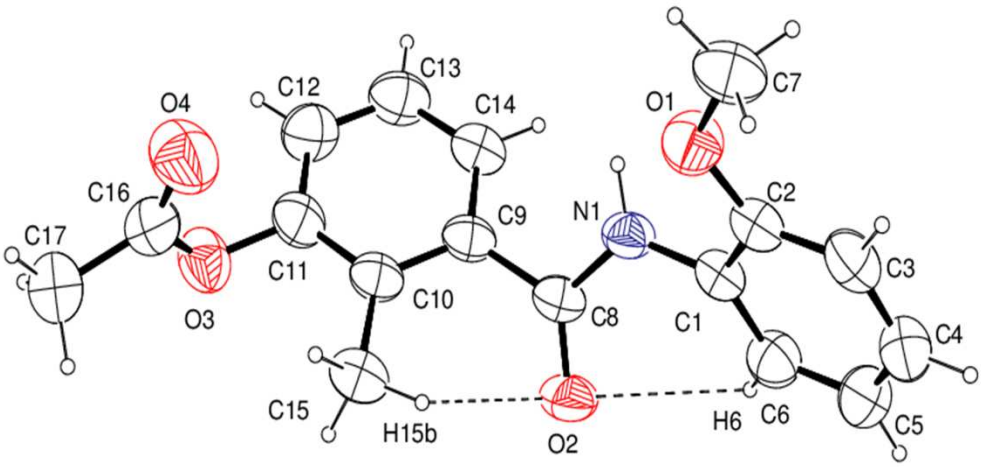

Figure 1. ORTEP-3 depiction of **1** with number scheme. The dashed bonds are the intramolecular hydrogen bonds.

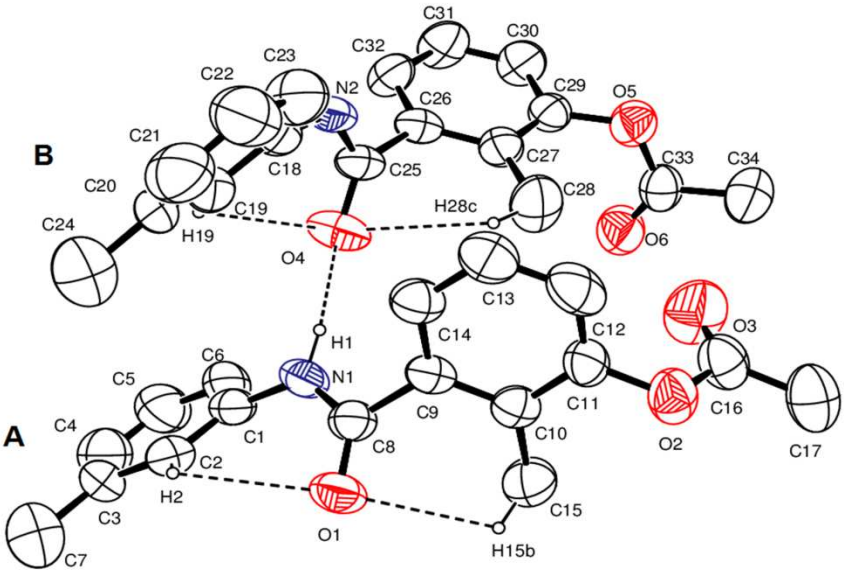

Figure 2. ORTEP-3 depiction of **2** with number scheme. The dashed bonds indicate the intramolecular hydrogen bonds and the hydrogen bonding in asymmetric unit. For clarity, hydrogen atoms not involved in hydrogen bonding were omitted.

There are two crystallographically independent molecules in the asymmetric unit of **2** (named molecule **A** and molecule **B**). Molecular geometries of **1** and **2** are not planar and the dihedral angles between the planes P1, P2 and P3 are listed in Table 2. P1, P2 and P3 are the planar groups which form the molecular structure (see Figure s1 at supplementary materials).

Table 2. Dihedral angles between planes P1, P2 and P3 for **1** and **2** (°).

Molecule	**P1-P2**	**P2-P3**	**P1-P3**
1	53.84	37.01	89.30
2A	58.93	39.24	82.03
2B	73.02	36.82	70.32

The molecular conformations are also affected by intermolecular and intramolecular hydrogen bonds, van der Waals interactions, C-H…π and π…π interactions. Both the crystal packing of compound **1** and the crystal packing of compound **2** contain intermolecular

hydrogen bonds, C-H…π interactions and weak van der Waals interactions in their own three-dimensional networks.

The crystal packing of **1** appears to be stabilized by two intramolecular C-H…O bonds, intermolecular N-H…O and C-H…O hydrogen bonds and two C-H…π interactions. While the intramolecular C6-H6…O2 [with D…A distance: 2.9095(8) Å] and C15-H15B…O2 [3.0345 (8) Å] bonds which can be seen from Fig. 1 form two pseudo six-membered rings of N(6) graph-set motif, the intermolecular N1-H1…O2^{i} [3.0014 (8) Å, symmetry code: (i) 1+x, y, z] and C17-H17A…O4^{ii} [3.5044 (8) Å, symmetry code: (ii) -1+x, y, z] bonds form hydrogen-bonded $R_2^2(20)$ motifs according to Graph-Set Notation [30]. It shows the formation of these motifs parallel to bc-plane of the unit cell. C7-H7C…*Cg(1)*^{i} [3.5743 (10) Å, symmetry code: (i) 1+x, y, z] and C14-H14…*Cg(2)*^{ii} [3.6563 (10) Å, symmetry code: (ii) -1+x, y, z] bonded chain structure of **1** along the a-axis of the unit cellis (see Figures s2 and s3 at supplementary materials).

The crystal packing of **2** appears to be stabilized by four intramolecular C-H…O bonds, an N-H…O hydrogen bond in asymmetric unit, an intermolecular N-H…O bond, two intermolecular C-H…O bonds and two C-H…π interactions. The N1-H1…O4 [2.8633 (3) Å] hydrogen bond which links two independent identical molecules in asymmetric unit, intermolecular N2-H2A…O1^{iii} [2.8531 (3) Å, symmetry code: (iii) x, 1+y, z], C12-H12…O6^{iv} [3.3874 (3) Å, symmetry code: (iv) -1+x, y, z] and C17-H17B…O3^{v} [3.4067 (3) Å, symmetry code: (v) 1-x, -y, 1-z] bonds can be seen (see Figure s4 at supplementary materials). Among these bonds, C17-H17B…O3^{v} forms a $R_2^2(8)$ motif. All these intermolecular hydrogen bonds in compound **2** connect the molecules along all directions and form a complex bonding motif. The C14-H14…*Cg(3)* [3.6539 (3) Å] (in asymmetric unit) and C32-H32…*Cg(1)*^{iii} [3.6759 (3) Å] interactions generate a chain motif along b-axis of the

unit cell (see Figure s5 at supplementary materials). Very similar intermolecular interactions can be seen from the previous paper [31].

The contact distances, angles, and the other details of intramolecular and intermolecular hydrogen bonds are summarized in Table 3.

Table 3. Hydrogen bonding geometry for **1** and **2** (Å, °).

D-H…A	**D-H** (Å)	**H…A** (Å)	**D…A** (Å)	**D-H…A**(°)
1				
C6-H6…O2	0.93	2.49	2.9095 (8)	108
C15-H15B…O2	0.96	2.41	3.0345 (8)	122
N1-H1…O2^{i}	0.86	2.18	3.0014 (8)	159
C17-H17A…O4^{ii}	0.96	2.58	3.5044 (8)	163
C7-H7…*Cg(1)*^{i}	0.93	2.69	3.5743 (10)	154
C14-H14…*Cg(2)*^{ii}	0.93	2.76	3.6563 (10)	156
2				
C2-H2…O1	0.93	2.59	2.9816 (3)	106
C15-H15B…O1	0.96	2.37	3.0383 (3)	126
C19-H19…O4	0.93	2.56	2.9665 (3)	107
C28-H28C…O4	0.96	2.59	3.2071 (3)	126
N1-H1…O4	0.86	2.05	2.8633 (3)	158
N2-H2A…O1^{iii}	0.86	2.06	2.8531 (3)	154
C12-H12…O6^{iv}	0.93	2.48	3.3874 (3)	167
C17-H17B…O3^{v}	0.96	2.54	3.4067 (3)	150
C14-H14…*Cg(3)*	0.93	2.79	3.6539 (3)	155
C31-H31…*Cg(4)*^{iii}	0.93	2.94	3.6759 (3)	137

^{i}[1+x, y, z], ^{ii}[-1+x, y, z], ^{iii}[x,1+y,z], ^{iv}[-1+x, y, z], ^{v}[1-x, -y, 1-z].
Cg(1): ring C1/C6 of **1**, *Cg(2)*: ring C9/C14 of **1**, *Cg(3)*: ring C18/C23 of **2**, *Cg(4)*: ring C1/C6 of **2**.

Some selected bond lengths and angles are listed in Table 4. The C-N and C=O bond lengths in the amide group of molecules fall within expected values and the good agreement can be seen between these bond lengths and angles with the counterparts in similar amide compounds [24, 25, 31-35].

Table 4. Selected geometrical parameters for **1** and **2** (Å, °).

1		**2A**		**2B**	
C8=O2	1.2218 (17)	C8=O1	1.220 (5)	C25=O4	1.224 (5)
C8-N1	1.3435 (19)	C8-N1	1.339 (6)	C25-N2	1.337 (6)
N1-C1	1.4165 (18)	N1-C1	1.426 (6)	N2-C18	1.446 (7)
C8-C9	1.504 (2)	C8-C9	1.508 (6)	C25-C26	1.500 (7)
C2-O1	1.3633 (18)	C11-O2	1.406 (6)	C29-O5	1.407 (6)
O1-C7	1.4177 (19)	O2-C16	1.373 (7)	O5-C23	1.360 (6)
C11-O3	1.4027 (19)	C16=O3	1.179 (6)	C33=O6	1.188 (5)
C16-O3	1.354 (2)	-	-	-	-
C16=O4	1.196 (2)	-	-	-	-
C9-C8-N1	114.92 (12)	C9-C8-N1	114.8 (4)	C26-C25-N2	114.8 (4)
C9-C8-O2	121.68 (13)	C9-C8-O1	120.8 (5)	C26-C25-O4	121.9 (4)
O2-C8-N1	123.40 (14)	O1-C8-N1	124.5 (4)	O4-C25-N2	123.3 (5)
C8-N1-C1	123.23 (12)	C8-N1-C1	126.6 (4)	C25-N2-C18	127.6 (4)

It is well known that the aromaticity is a sign of more delocalized electron clouds, and the delocalization of electrons gives more stability to the molecules. Beside the delocalization, *trans* configuration of main groups of molecules is another factor which gives additional stability to the molecule. In *trans* configuration steric interactions between the hydrogen atoms are less effective than that of *cis* configuration. Molecules have two six-membered rings which are in *trans* configuration with respect to amide C-N bonds. The harmonic oscillator model of aromaticity (HOMA) index gives information about the aromaticity of compounds and is based upon average squared deviation of bond lengths. HOMA index has been calculated for both rings of **1** and **2** by using following equation [36, 37] because we observed that the bond lengths in one of the rings in molecule **2B** are very different from each other.

$$\mathrm{HOMA} = 1 - \left[\frac{1}{n}\sum_{i=1}^{n}\alpha_i(R_i - R_{opt})^2\right] \quad (1)$$

Where n is the number of bonds in the molecular fragments of interest (in our case n is equal to 6 for the six-membered rings), α_i normalization constant is equal to 257.7, R_i is individual bond length and R_{opt} is equal to 1.388 Å for C-C bonds in an aromatic ring. For the purely aromatic systems the HOMA index is equal to 1 and for the non-aromatic ones equal to 0. The calculated indices are found as 0.974 for C1/C6 ring (ring containing atoms C1 to C6, hereafter abbreviated C1/C6 ring) and 0.976 for C9/C14 ring (ring containing atoms C9 to C14) of **1**, 0.727 for C1/C6 ring, 0.961 for C9/C14 ring of **2A** and 0.322 for C18/C23 ring (ring containing atoms C18 to C23), 0.937 for C26/C32 ring (ring containing atoms C26 to C32) of **2B**. There is one slight andone considerable deviation from the aromaticity for the six membered rings in compound **2**. The slight deviation belongs to C1/C6 ring of **2A** but the ring can still be defined as aromatic. On the other hand, C18/C23 ring of **2B** appears to show a somewhat reduced degree of aromaticity in the solid state. The C-H… π interaction including the C18/C23 ring and the hyperconjugative resonance effect with the methyl group must be responsible for the deviations.

3.2. Electronic structures

For all the DFT calculations, B3LYP hybrid exchange-correlation functional [38,39] has been employed with 6-311+G(d,p) basis set [40] as implemented in Gaussian03 package [41].

The electron delocalization gives amides a polar character, and because of this polar character, amides forms relatively strong hydrogen bonds involving both their C=O group and N-H proton [42]. In this part of the study, we examine the electronic delocalization and electrostatic potential surfaces on the basis of natural bond orbital (NBO) analyses and molecular electrostatic potential (MEP) plots of compounds **1** and **2** with the help of density functional theory (DFT) to investigate the above-mentioned hydrogen bondings.

The electron delocalization can be rationalized well by the NBO analysis which gives the stabilization energy and the redistribution of electron density in bonding and antibonding orbitals. The NBO calculations were performed using NBO 3.1 program [43] as implemented in the Gaussian 03W package on the optimized geometries of compounds **1** and **2**. In this method, the stabilization energy E(2) associated with the delocalization i→j for each donor (i) and acceptor (j) is defined with the following equation:

$$E(2) = q_i \frac{(F_{ij})^2}{(E_j - E_i)} \qquad (2)$$

where q_i is the donor orbital occupancy, E_i and E_j are the diagonal and F_{ij} is the off-diagonal elements of the Fock matrix (orbital energies) [44, 45]. The larger E(2) values indicate the stronger interactions between electron-donors and acceptors and larger extent of conjugation of the whole system. Table 5 summarizes the possible intensive interactions (which the stabilization energies are larger than 15 kcal/mol) for compound **1** and **2**.

Table 5. Electron delocalization and second order interaction energies for **1** and **2**.

	Donor (i)	Acceptor (j)	E(2) (kcal/mol)	E_j-E_i (a.u.)	F_{ij} (a.u.)
1					
	π(C1-C6)	π*(C2-C3)	20.65	0.28	0.068
	π(C1-C6)	π*(C4-C5)	19.07	0.29	0.067
	π(C2-C3)	π*(C1-C6)	16.54	0.30	0.064
	π(C2-C3)	π*(C4-C5)	18.93	0.30	0.068
	π(C4-C5)	π*(C1-C6)	20.07	0.28	0.068
	π(C4-C5)	π*(C2-C3)	18.83	0.27	0.065
	π(C9-C14)	π*(C10-C11)	20.38	0.29	0.069
	π(C9-C14)	π*(C12-C13)	18.65	0.30	0.067
	π(C10-C11)	π*(C9-C14)	19.80	0.29	0.067
	π(C10-C11)	π*(C12-C13)	20.47	0.30	0.071
	π(C12-C13)	π*(C9-C14)	20.62	0.29	0.069
	π(C12-C13)	π*(C10-C11)	20.69	0.29	0.069

n1(N1)	π*(C1-C6)	34.04	0.30	0.090
n1(N1)	π*(C8-O2)	50.02	0.30	0.112
n2(O1)	π*(C2-C3)	26.79	0.35	0.093
n2(O2)	σ*(C8-C9)	18.54	0.66	0.100
n2(O2)	σ*(C8-N1)	25.08	0.70	0.120
n2(O4)	σ*(C16-C17)	17.62	0.64	0.098
n2(O4)	σ*(C16-O3)	36.04	0.61	0.134
2				
π(C1-C2)	π*(C3-C4)	22.14	0.29	0.072
π(C1-C2)	π*(C5-C6)	18.05	0.28	0.064
π(C3-C4)	π*(C1-C2)	18.49	0.28	0.064
π(C3-C4)	π*(C5-C6)	23.78	0.27	0.072
π(C5-C6)	π*(C1-C2)	20.77	0.29	0.070
π(C5-C6)	π*(C3-C4)	16.27	0.30	0.063
π(C9-C10)	π*(C11-C12)	21.03	0.29	0.068
π(C9-C10)	π*(C13-C14)	21.63	0.30	0.070
π(C11-C12)	π*(C9-C10)	20.92	0.30	0.071
π(C11-C12)	π*(C13-C14)	19.80	0.29	0.068
π(C13-C14)	π*(C9-C10)	19.50	0.29	0.068
π(C13-C14)	π*(C11-C12)	20.28	0.28	0.068
n1(N1)	π*(C1-C2)	33.16	0.30	0.090
n1(N1)	π*(C8-O1)	48.24	0.31	0.111
n2(O1)	σ*(C8-C9)	18.56	0.66	0.100
n2(O1)	σ*(C8-N1)	25.39	0.70	0.121
n2(O3)	σ*(C16-C17)	17.60	0.64	0.098
n2(O3)	σ*(C16-O2)	35.07	0.61	0.132

In Table 5, first twelve lines for both **1** and **2** are about the electron delocalization in the phenyl rings of compounds. These are expected donor – acceptor interactions because of the aromaticity of phenyl rings which they give additional stability to the compounds. The stabilization energy values for these expected π(C-C) → π*(C-C) intramolecular charge transfers are in the range of 16 kcal/mol - 20 kcal/mol. The strongest interaction for **1** is the electron donation that forms the donor lone pair n1(N1) orbitalto the π*(C8-O2) anti-bonding

orbital with the 50.02 kcal/mol stabilization energy which contributes to a resonance interaction in the amide group of molecules. The other significant contibutions in second order perturbation approach table for **1** is n2(O4) → σ*(C16-O3), n1(N1) → π*(C1-C6) and n2(O2) → σ*(C8-N1) with the stabilization energies of 36.04, 34.04 and 25.08 kcal/mol, respectively. The similar donor – acceptor interactions occured in compound **2** according to the second order perturbation theory analysis of **2**. Beside the π(C-C) → π*(C-C) interactions, there are four more noteworthy donations attract the attention in Table 5. The strongest one is the electron donation that forms the donor lone pair n1(N1) orbital to the anti-bonding π*(C8-O1) orbital in the amide group with the 48.24 kcal/mol stabilization energy. The others are n2(O3) → σ*(C16-O2), n1(N1) → π*(C1-C2) and n2(O1) → σ*(C8-N1) with the stabilization energies of 35.07, 33.16 and 25.39 kcal/mol, respectively. NBO analyses of **1** and **2** reveal that the electron delocalizations in amide groups make these groups more polar, the oxygen and NH proton becomes much better hydrogen bond acceptors and donors.

The charge density and chemical reactivity, so also the relative polarity of a molecule can be understood well by looking at the molecular electrostatic potential (MEP) map which represents different values of electrostatic potential with different colours [46]. MEPs are drawn onto the constant electron density surface. On these maps, while blue colour represents the most positive regions which have the strongest attraction, red colour is for the most electronegative regions which indicate the strongest repulsion. The MEPs of title compounds are presented in Figures 3 and 4 for compound **1** and **2**, respectively. The colour scales on the maps show the lower and upper limits of electrostatic potentials. The electrostatic potential is in the range between -5.452×10^{-2} a.u. and 5.452×10^{-2} a.u. for compound **1** and in the range between -6.527×10^{-2} a.u. and 6.527×10^{-2} a.u. for compound **2**. The figures clearly show that the MEPs of two investigated compounds are very similar. In both maps, the most positive regions are localized on the hydrogen atoms bonded to nitrogens of amide groups. On the

other hand, the most negative regions are on the C=O oxygens. These results are in agreement with the well-known fact that the negative regions of MEPs are associated with the lone electron pairs of the electronegative atoms in general. The obtained results are also in accordance with NBO data.

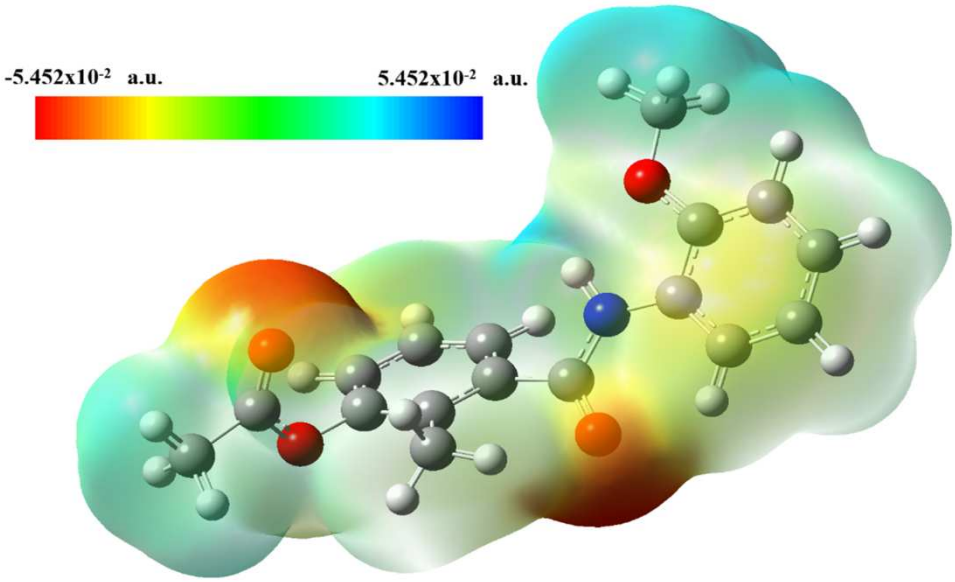

Figure 3. MEP of title compound **1**.

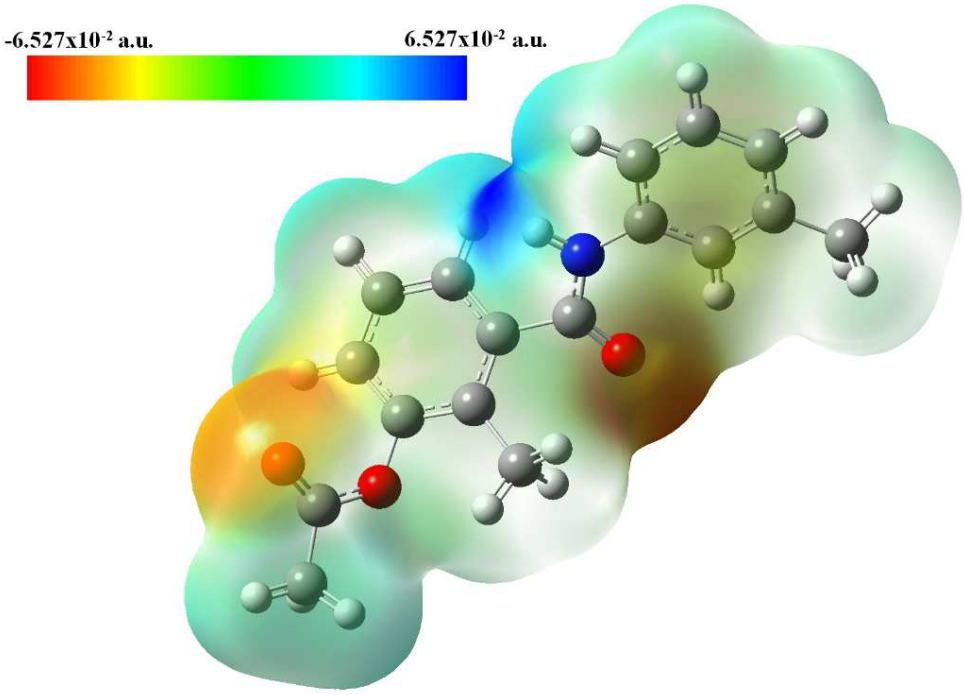

Figure 4. MEP of title compound **2**.

We have also calculated the NLO (non-linear optical) properties like linear polarizability (α) and the first-order hyperpolarizability (β) values of the title compounds with the help of DFT because of their good transfer of charges which can be seen from the NBO analyses results. The NLO properties of a compound have an important role for design of new materials in optical technology, for example signal processing and optical interconnection devices. Because of their π-electron cloud movement, especially organic molecules have larger NLO susceptibilities [47]. In order to obtain the α and β values of the compounds, the components of linear polarizability and the first-order hyperpolarizability have been calculated using polar=ENONLY input to Gaussian03 at the level of B3LYP/6-31+G(d,p) in the gas phase and the components have been used in the following equations: [48]

$$\alpha = \frac{1}{3}\left[\alpha_{xx} + \alpha_{yy} + \alpha_{zz}\right] \tag{3}$$

$$\beta = \left[\begin{array}{c}(\beta_{xxx}+\beta_{xyy}+\beta_{xzz})^2 + \\ (\beta_{yyy}+\beta_{xxy}+\beta_{yzz})^2 + \\ (\beta_{zzz}+\beta_{xxz}+\beta_{yyz})^2\end{array}\right]^{1/2} \tag{4}$$

The calculated α and β values are 230.762 $Å^3$ and 3.716×10^{-30} cm^5/esu for compound **1**, 224.567 $Å^3$ and 3.513×10^{-30} cm^5/esu for compound **2**. In order to understand whether the compound is a good candidate for non-linear optical studies or not, we compared the linear polarizability and the first-order hyperpolarizability values with those of urea as a common way in literature. For urea with the same functional and basis set by DFT method, calculated α and β values were found as 3.831 $Å^3$ and 0.373×10^{-30} cm^5/esu [49]. In our ongoing work, while β of compound **1** is 9.96 times greater than that of urea, β of compound **2** is 9.41 times greater than that of urea. These values are relatively high when compared to the literature [50, 51] and point out that both compound **1** and **2** can be good candidates for non-linear optical materials.

3.3. Vibrational frequencies

In the IR spectra, characteristic amide bands were observed for the compounds (see Figure s6 at supplementary materials). The N–H stretching vibration was observed as characteristic absorption at 3323 cm^{-1} for compound **1**. In compound **2**, the same band appeared at 3234 cm^{1}. In compounds **1** and **2**, the C=O (amide I) stretching vibrations were observed as second characteristic absorption band at 1660 cm^{-1} and 1651 cm^{-1}, respectively. For compounds **1** and **2**, the C=O stretching vibration of ester carbonyl groups were observed very strong vibrational bands at 1750 cm^{-1} and 1761 cm^{-1}, respectively. The strong C=O stretching vibration of ester carbonyl group was observed at higher wavenumber than the normal stretching vibration of aliphatic ester (~1740 cm^{-1}) due to resonance of the phenyl group with oxygen. Another group wavenumber was the C-N stretching vibration with the N-H bending vibration (amide II) resulting from Fermi resonance effect. In compounds **1** and **2**, this mode was observed at 1458 cm^{-1} and 1455 cm^{-1} in the infrared spectra, respectively. These data are in agreement with those both previously reported for similar compounds [25, 52].

3.4. NMR spectra

The ^{1}H NMR spectrum of compound **1** was recorded in $CDCl_3$ [Fig. 5]. While the three methyl protons attached to ester carbonyl was resonated at 2.38 ppm (s, 3H, $-OCOCH_3$) as a singlet, three protons due to methyl group at 2-position on the phenyl ring were observed at 2.35 ppm (s, 3H, $ArCH_3$) as a singlet. The signal was observed at 3.89 ppm (s, 3H, $ArOCH_3$) due to the methoxy group at 2′-position of the phenyl ring. The signal of NH proton appeared as a singlet at 8.15 ppm (s, 1H, NH-C=O) which was very characteristic for this type of amide protons. For compound **1**, the aromatic protons of the phenyl rings appeared in the region of δ= 6.92-7.42 ppm [Fig. 5].

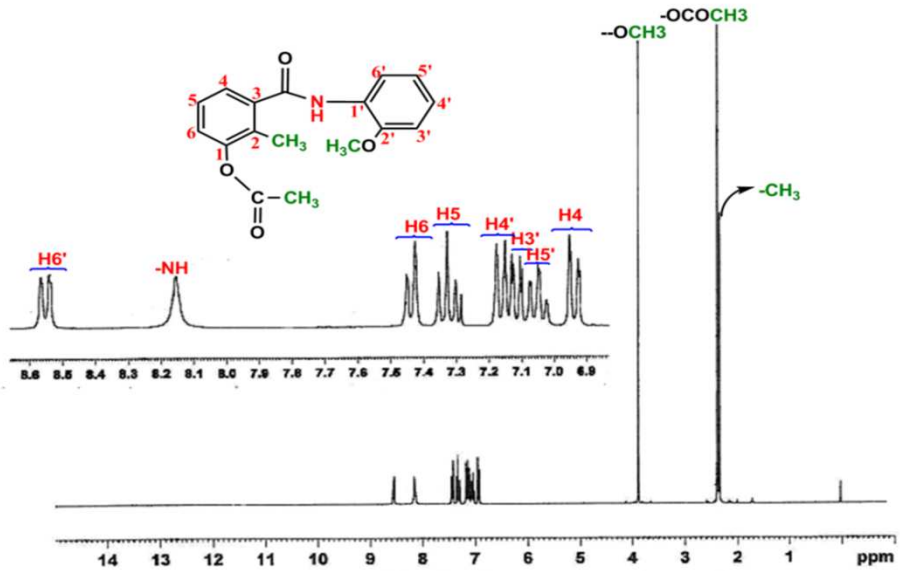

Figure 5. ^{1}H NMR spectrum of compound **1**.

This compound was further characterized by ^{13}C NMR [Fig. 6]. The ^{13}C NMR spectrum of compound **1** showed 17 distinct resonances in agreement with the proposed structure. The carbon atom of the ester carbonyl group appeared at 169.4 ppm, whereas the amide carbonyl functional group was observed at 167.0 ppm. The aromatic C1 and C2′ carbons were the most downfield in comparison with the other carbons of the aromatic rings and so these carbons gave the signal at 149.9 ppm and 148.1 ppm respectively. This downfield shift was due to the presence of acetoxy group at the 1-position in the aromatic ring and the methoxy group at 2′-position of the other phenyl ring. The other carbons of the aromatic rings (C2, C3, C4, C5, C6, C1′, C3′, C4′, C5′ and C6′) were at 127.6 ppm, 138.9 ppm, 126.9 ppm, 128.9 ppm, 124.2 ppm, 124.7 ppm, 119.8 ppm, 126.9 ppm, 124.0 ppm and 121.1 ppm, respectively. The methyl carbon attached to ester carbonyl group (-$OCOCH_3$) gave a signal at 20.8 ppm, while the signal at 13.0 ppm belonged to methyl group carbon (-CH_3) located at 2-position on the phenyl ring. The methyl carbon attached to methoxy group (-OCH_3) at 2′-position of the phenyl ring gave a signal at 55.6 ppm. These values are in agreement with the values of previously reported for similar compounds [25].

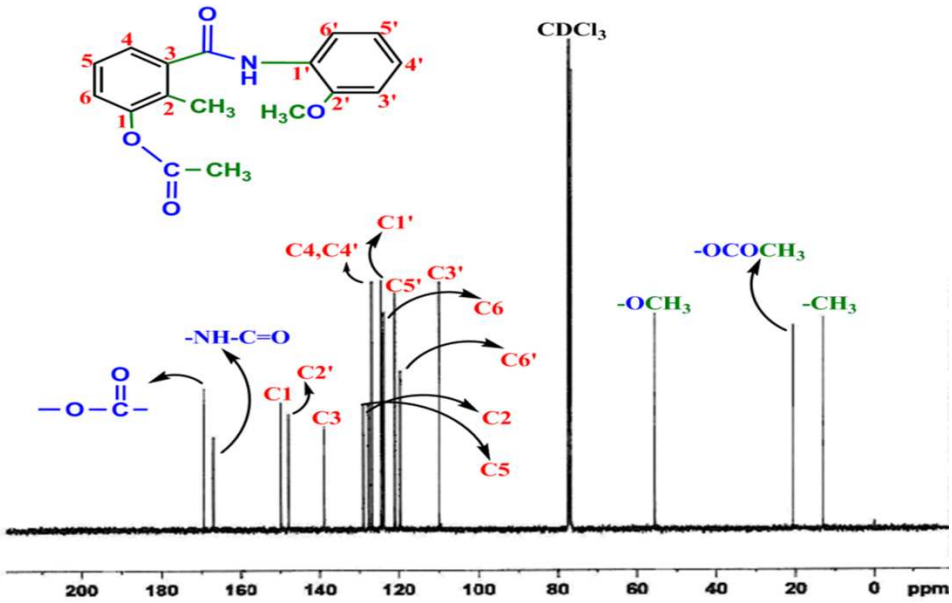

Figure 6. ^{13}C NMR spectrum of compound **1**.

The ^{1}H NMR spectrum of compound **2** was recorded in $CDCl_3$ [Fig. 7]. The methyl group protons at the 3′- and 2-positions of phenyl rings were observed as two different singlets at 2.30 and 2.34 ppm for compound **2**. The methyl proton of ester carbonyl group was observed at 2.38 ppm. The proton of the amide group (NH-C=O) also appeared as a singlet at 7.64 ppm. Aromatic protons of phenyl ring appeared in the region of 7.10-7.50 ppm. The H2′ proton showed a singlet at 7.50 ppm. The H4′ proton coupled to H5′ proton and gave doublet peak at 6.99 ppm.

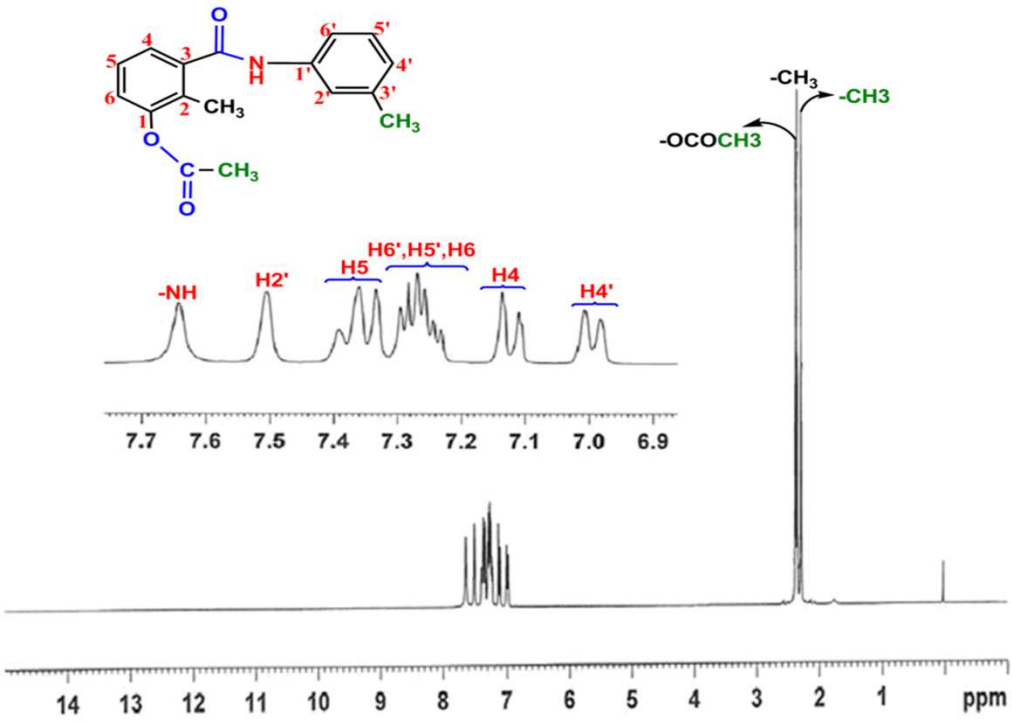

Figure 7. ^{1}H NMR spectrum of compound **2**.

The ^{13}C NMR spectrum of compound **2** was recorded in $CDCl_3$ [Fig. 8]. The chemical structure was confirmed by the presence of 17 peaks, as expected. The ^{13}C NMR spectrum of compound **2** displayed a peak at 21.5 ppm, which was consistent with methyl group carbon at 3′-positionon the phenyl ring. The other two methyl carbons were attached to ester carbonyl group (-$OCOCH_3$) and were located at 2-positions of phenyl ring resonate at 20.8 ppm and 13.0 ppm, respectively. The carbon of ester carbonyl group appeared at 169.3 ppm, whereas the amide carbonyl functional group was observed at 167.2 ppm. The aromatic C1 carbon bearing the acetoxy group (-$OCOCH_3$) and the aromatic C3′ carbon of phenyl ring was the most deshielded carbons, and so these carbons gave the signals which were the furthest downfield at 149.90 ppm and 139.09 ppm respectively. The rest of aromatic carbon signals were observed between 138.7-117.0 ppm. These results are consistent with the literature values [25].

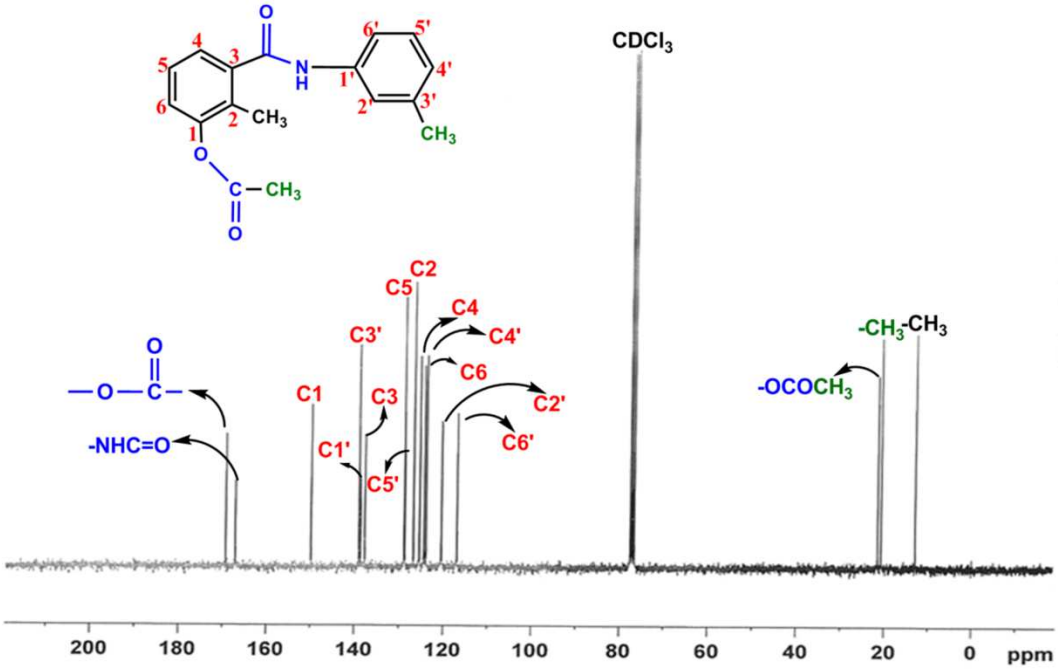

Figure 8. ^{13}C NMR spectrum of compound **2**.

4. Conclusions

In the present work, we have described the syntheses and characterizations of two secondary amide compounds 3-acetoxy-2-methyl-*N*-(2-methoxyphenyl) benzamide and 3-acetoxy-2-methyl-*N*-(3-methylphenyl) benzamide by using the X-ray diffraction, IR, ^{1}H NMR and ^{13}C NMR techniques experimentally and by using DFT theoretically. The results of X-ray studies showed that the six-membered rings are in *trans* configuration with respect to C-N bond of amide bridge in both molecules. The intramolecular and intermolecular hydrogen bonds and C-H…π interactions stabilized the crystal structures of compounds **1** and **2**. According to the FT-IR and NMR results, characteristic absorption bands and NMR signals are in the expected ranges for the amide structures. MEP and NBO studies carried out by DFT method are qualified to explain the hydrogen bondings in compounds. Calculated linear polarizability and first-order hyperpolarizability values of compounds indicated that they can be considered as potential non-linear optical materials. We hope that the results of this study will be helpful for the further studies.

Conflict of Interest: The authors declare that they have no conflict of interest.

Acknowledgements

We would like to thank Ondokuz Mayis University (Grant No. PYO.FEN.1904.12.007) for its financial support of this work.

References

[1] E. Valeur, M. Bradley, Amide bond formation: beyond the myth of coupling reagents, Chem. Soc. Rev. 38 (2009) 606-631.

[2] J.K. Park, W.K. Shin, D.K. An, New and efficient synthesis of amides from acid chlorides using diisobutyl (amino) aluminum, Bull. Korean Chem. Soc. 34 (2013) 1592-1594.

[3] A. Khalafi-Nezhad, A. Parhami, M.N. Soltani Rad, A. Zarea, Efficient method for the direct preparation of amides from carboxylic acids using tosyl chloride under solvent-free conditions, Tetrahedron Lett. 46 (2005) 6879-6882.

[4] R.M. Lanigan, P. Starkov, T.D. Sheppard, Direct synthesis of amides from carboxylic acids and amines using $B(OCH_2CF_3)_3$, J. Org. Chem. 78 (2013) 4512-4523.

[5] V.R. Pattabiraman, J.W. Bode, Rethinking amide bond synthesis, Nature 480 (2011) 471-479.

[6] R.M. Srivastava, R.A.W. Neves Filho, C.A. da Silva, A.J. Bortoluzzi, First ultrasound-mediated one-pot synthesis of *N*-substituted amides, Ultrason Sonochem. 16 (2009) 737-742.

[7] A.L.J. Beckwith, J. Zabicky, The chemistry of amides. Synthesis of amides, Interscience Publishers: London (1970) 105-109.

[8] J.W. Bode, Emerging methods in amide-and peptide-bond formation. Curr. Opin. Drug Disc. 9(6) (2006) 765-775.

[9] R. Tang, L. Jin, C. Mou , J. Yin , S. Bai , D. Hu , J. Wu , S. Yang, B. Song, Synthesis, antifungal and antibacterial activity for novel amide derivatives containing a triazole moiety, Chem. Cent. J. 7 (2013) 30-36.

[10] D. Rai, R.K. Singh, Synthesis and antibacterial activity of benzamides and sulfonamide derived from 2-amino-5-bromo/nitropyridine against bacterial strains isolated from clinical patients, Indian J. Chem. 50B(7) (2011) 931-936.

[11] N. Kushwaha, R.K. Saini, S.K.S. Kushwaha, Synthesis of some amide derivatives and their biological activity, Int. J. Chem. Tech. Res. 3 (2011) 203-209.

[12] J. Fu, K. Cheng, Z.M. Zhang, R.Q. Fang, H.L. Zhu, Synthesis, structure and structure–activity relationship analysis of caffeic acid amides as potential antimicrobials, Eur. J. Med. Chem. 45 (2010) 2638-2643.

[13] S. Nadeem, M. Shamsher-Alam, W. Ahsan, Synthesis, anticonvulsant and toxicity evaluation of 2-(*1H*-indol-3-yl) acetyl-*N*-(substituted phenyl) hydrazine carbothioamides and their related heterocyclic derivatives, Acta Pharma 58 (2008) 445-454.

[14] D. Carbonnelle, F. Ebstein, C. Rabu, J.Y. Petit, M. Gregoire, F. Lang, A new carboxamide compound exerts immuno□suppressive activity by inhibiting dendritic cell maturation, Eur. J. Immunol. 35 (2005) 546-556.

[15] Y.F. Xiang, C.W. Qian, G.W. Xing, J. Hao, M. Xia, Y.F. Wang, Anti-herpes simplex virus efficacies of 2-aminobenzamide derivatives as novel HSP90 inhibitors, Bioorg. Med. Chem. Lett. 22 (2012) 4703-4706.

[16] F.A. Bettelheim, J. March, *Introduction to General, Organic and Biochemistry*, (Sounders College Publishing: Fort Worth) 5th Ed. p 492-508, 1998.

[17] Y. Nagaoka, T. Maeda, Y. Kawai, D. Nakashima, T. Oikawa, K. Shimoke, T. Ikeuchi, H. Kuwajima, S. Uesato, Synthesis and cancer antiproliferative activity of new histone

deacetylase inhibitors: hydrophilic hydroxamates and 2-aminobenzamide-containing derivatives, Eur. J. Med. Chem. 41 (2006) 697-708.

[18] K. Suzuki, H. Nagasawa, Y. Uto, Y. Sugimoto, K. Noguchi, M. Wakida, K. Wierzba, T. Terada, T. Asao, Y. Yamada, K. Kitazato, H. Hori, Napthalimidobenzamide DB-51630: a novel DNA binding agent inducing p300 gene expression and exerting a potent anti-cancer activity, Bioorg. Med. Chem. 13 (2005) 4014-4021.

[19] Y. Liu, G.Y. Zhang, Y. Li, Y.N. Zhang, S.Z. Zheng, Z.X. Zhou, S.J. An, Y.H. Jin, Synthesis of novel amide derivatives with in vitro antiproliferative and cytotoxic activity, Heteroat. Chem. 24 (2013) 9-17.

[20] A.K. Srivastava, A.K. Pandey, B. Narayana, B.K. Sarojini, P.S. Nayak, N. Misra, Normal modes, molecular orbitals and thermochemical analyses of 2,4 and 3,4-dichloro substituted phenyl-*N*-(1,3-thiazol-2-yl) acetamides: DFT study and FTIR spectra, J. Theoretical Chem. (2014) 1-10.

[21] A. Padmaja, K. Laxmi, R.R. Palreddy, S.D. Choudhary, A study on structural aspects and biological activity of (E)-*N′*-[2-hydroxybenzylidene] benzohydrazide and its metal complexes, J. Applied Chem. 12 (2014) 12-22.

[22] B.G. Johnson, P.M.W. Gill, J.A. Pople, The performance of a family of density functional methods, J. Chem. Phys. 98 (1993) 5612-5626.

[23] P.M.W. Gill, B.G. Johnson, J.A. Pople, M.J. Frisch, The performance of the Becke-Lee-Yang-Parr (B-LYP) density functional theory with various basis sets, J. Chem. Phys. Lett. 197 (1992) 499-505.

[24] Ş. Çakmak, H. Kütük, M. Odabaşoğlu, H. Yakan, O. Büyükgüngör, Spectroscopic properties and preparation of some 2, 3-dimethoxybenzamide derivatives, Lett. Org. Chem. 13 (2016) 181-194.

[25] S. Demir, Ş. Çakmak, N. Dege, H. Kütük, M. Odabaşoğlu, A novel 3-acetoxy-2-methyl-*N*-(4-methoxyphenyl) benzamide: Molecular structural describe, antioxidant activity with use X-ray diffractions and DFT calculations, J. Mol. Struct. 1100 (2015) 582-591.

[26] Stoe&Cie, X-AREA (Version 1.18) and X-RED32 (Version 1.04), Darmstadt, Germany, 2002.

[27] G.M. Sheldrick, SHELXT – Integrated space-group and crystal-structure determination, Acta Cryst. A71 (2015) 3-8.

[28] G.M. Sheldrick, Crystal structure refinement with SHELXL, Acta Cryst. C71 (2015) 3-8.

[29] L.J. Farrugia, ORTEP-3 for Windows-a version of ORTEP-III with a Graphical User Interface (GUI), J. Appl. Cryst. 30 (1997) 565-566.

[30] M.C. Etter, J.C. MacDonald, J. Bernstein, Graph-set analysis of hydrogen-bond patterns in organic crystals, Acta Cryst. B46 (1990) 256-262.

[31] B.K. Kırca, Ş. Çakmak, H. Kütük, M. Odabaşoğlu, O. Büyükgüngör, Synthesis and characterization of 3-acetoxy-2-methyl-*N*-(phenyl) benzamide and 3-acetoxy-2-methyl-*N*-(4-methylphenyl) benzamide, J. Mol. Struct. 1151 (2018) 191-197.

[32] A. Atilgan, Ş. Yurdakul, Y. Erdogdu, M.T. Güllüoğlu, DFT simulation, quantum chemical electronic structure, spectroscopic and structure-activity investigations of 4-acetylpyridine, J. Mol. Struct. 1161 (2018) 55-65.

[33] V.N. Sonar, S. Parkin, P.A. Crooks, The effect of hydrogen bonding on the conformations of 2-(1H-indol-3-yl)-2-oxoacetamide and 2-(1H-indol-3-yl)-*N*,*N*-dimethyl-2-oxoacetamide, Acta Crystallogr C. 68(10) (2012) o405-o407.

[34] L. Hennig, K. Ayala-Leon, J. Angulo-Cornejo, R. Richter, L. Beyer, Fluorine hydrogen short contacts and hydrogen bonds in substituted benzamides, J. Fluor. Chem. 130 (2009) 453-460.

[35] P. Prabukanthan, R. Lakshmi, G. Harichandran, C. Sudarsana Kumar, Synthesis, structural, optical and thermal properties of *N*-methyl–*N*-aryl benzamide organic single crystals grown by a slow evaporation technique, J. Mol. Struct. 1156 (2018) 62-73.

[36] J. Kruszewski, T.M. Krygowski, Definition of aromaticity basing on the harmonic oscillator model, Tetrahedron Lett. 13 (1972) 3839-3842.

[37] T.M. Krygowski, M.K. Cyrański, Structural aspects of aromaticity, Chem. Rev. 101 (2001) 1385-1419.

[38] C. Lee, W. Yang, R.G. Parr, Density-functional exchange-energy approximation with correct asymptotic behavior, Phys. Rev. B37 (1988) 785-789.

[39] A.D. Becke, Becke's three parameter hybrid method using the LYP correlation functional, J. Chem. Phys. 98 (1993) 5648-5652.

[40] R. Ditchfield, W.J. Hehre, J.A. Pople, Self□consistent molecular□orbital methods. IX. An extended Gaussian□type basis for molecular□orbital studies of organic molecules, J. Chem. Phys. 54 (1971) 724-728.

[41] M.J. Frisch, G.W. Trucks, H.B. Schlegel, G.E. Scuseria, M.A. Robb, J.R. Cheeseman, J.A. Montgomery Jr., T. Vreven, K.N. Kudin, J.C. Burant, J.M. Millam et al. Gaussian Inc., Wallingford, CT, 2004.

[42] J. Zabicky, *Amides*, John Wiley & Sons Ltd., 1970.

[43] E.D. Glendening, A.E. Reed, J.E. Carpenter, F. Weinhold, *NBO Version 3.1*, Theoretical Chemistry Institute, University of Wisconsin, Madison, 1998.

[44] S. Sebastian, N. Sundaraganesan, The spectroscopic (FT-IR, FT-IR gas phase, FT-Raman and UV) and NBO analysis of 4-Hydroxypiperidine by density functional method, Spectrochim. Acta A 75 (2010) 941–952.

[45] J. Karpagam, N. Sundaraganesan, S. Sebastian, S. Manoharan, M. Kurt, Molecular structure, vibrational spectroscopic, first□order hyperpolarizability and HOMO, LUMO studies of 3□hydroxy□2□naphthoic acid hydrazide, J. Raman Spectr. 41 (2010) 53–62.

[46] J.S. Murray, K. Sen, *Molecular Electrostatic Potentials, Concepts and Applications*, Elsevier, Amsterdam, 1976.

[47] L. Fang, G.C. Yang, Y.Q. Qui, Z.M. Su, Theoretical prediction of third-order optical nonlinearities of $[Al_4MAI_4]^{n-}$ (n=0-2, M=Ti, V and Cr) clusters, Theor. Chem. Account. 119 (2008) 329-333.

[48] D. Sajan, J. Hubert, V.S. Jayakumar, J. Zaleski, Structural and electronic contributions to hyperpolarizability in methyl p-hydroxy benzoate, J. Mol. Struct. 785 (2006) 43–53.

[49] a) Y.X. Sun, Q.L. Hao, W.X. Wei, Z.X. Yu, L.D. Lu, X. Wang, Y.S. Wang, Experimental and density functional studies on 4-(3, 4-dihydroxybenzylideneamino) antipyrine, and 4-(2, 3, 4-trihydroxybenzylideneamino) antipyrine, J. Mol. Struct. (Theochem) 904 (2009) 74-82.

b) K. Kumara, A.D. Kumar, S. Naveen, K.A. Kumar, N.K Lokanath, Synthesis, spectral characterization and X-ray crystal structure studies of 3-(benzo [*d*] [1,3] dioxol-5-yl)-5-(3-methylthiophen-2-yl)-4, 5-dihydro-1H-pyrazole-1-carboxamide: Hirshfeld surface, DFT and thermal analysis, J. Mol. Struct. 1161 (2018) 285-298.

c) S. Xavier, S. Periandy, S. Ramalingam, NBO, conformational, NLO, HOMO-LUMO, NMR and electronic spectral study on 1-phenyl-1-propanol by quantum computational methods, Spectrochim. Acta Part A: Mol. Biomol. Spectrosc. 137 (2015) 306-320.

[50] M. Raja, R. Raj Muhamed, S. Muthu, M. Suresh, Synthesis, spectroscopic (FT-IR, FT-Raman, NMR, UV–Visible), NLO, NBO, HOMO-LUMO, Fukui function and

molecular docking study of (E)-1-(5-bromo-2-hydroxybenzylidene) semicarbazide, J. Mol. Struct. 1141 (2017) 284-298.

[51] P. Bragiel, I. Radkowska, R. Belka, B. Marciniak, Z. Bak, Structural, spectroscopic and NLO features of the 4-chloro-1-naphthol, J. Mol. Struct. 1154 (2018) 27-38.

[52] A.G. Iríarte, M.F. Erben, K. Gholivand, J.L. Jios, S.E. Ulic, C.O. Della Védova, [Chloro (difluoro) acetyl] phosphoramidic acid dichloride $ClF_2CC(O)NHP(O)Cl_2$, synthesis, vibrational and NMR spectra and theoretical calculations, J. Mol. Struct. 886 (2008) 66-67.

Figure Captions

Scheme 1. Synthesis of compunds **1** and **2**.

Figure 1. ORTEP-3 depiction of **1** with number scheme. The dashed bonds are the intramolecular hydrogen bonds.

Figure 2. ORTEP-3 depiction of **2** with number scheme. The dashed bonds indicate the intramolecular hydrogen bonds and the hydrogen bonding in asymmetric unit. For clarity, hydrogen atoms not involved in hydrogen bonding were omitted

Figure 3. MEP of title compound **1**.

Figure 4. MEP of title compound **2**.

Figure 5. ^{1}H NMR spectrum of compound **1**.

Figure 6. ^{13}C NMR spectrum of compound **1**.

Figure 7. ^{1}H NMR spectrum of compound **2**.

Figure 8. ^{13}C NMR spectrum of compound **2**.

Highlights

- Syntheses of two new secondary amide compounds.
- The compounds were characterized by X-ray crystal diffraction and spectroscopic techniques.
- Quantum chemical calculations were used for the investigations on electronic structure.
- The intramolecular and intermolecular hydrogen bonds and C-H…π interactions.
- MEP and NBO studies which carried out by DFT method.

Declaration of interests

☒ The authors declare that they have no known competing financial interests or personal relationships that could have appeared to influence the work reported in this paper.

☐The authors declare the following financial interests/personal relationships which may be considered as potential competing interests: